Model-based Prototyping of a Controller for MR Actuators

Gabriel Mendes
Cracow University of Technology
Warszawska 24, 31-155 Krakow, Poland
gabriel.mendes@doktorant.pk.edu.pl

Janusz Gołdasz
Cracow University of Technology
Warszawska 24, 31-155 Krakow, Poland
janusz.goldasz@pk.edu.pl

Ângela Ferreira
CeDRI, Polytechnic Institute of Bragança
5300-252 Bragança, Portugal
apf@ipb.pt

2023 24th International Carpathian Control Conference (ICCC) | 979-8-3503-1022-1/23/$31.00 ©2023 IEEE | DOI: 10.1109/ICCC57093.2023.10178923

***Abstract*—Magnetorheological (MR) actuators are semi-active devices that leverage the smart properties of the MR fluids whose rheology can be controlled by an external magnetic field. Within the presence of an external magnetic field, the magnetic domains of the MR fluid align with the external field, which results in the yield stress induced in the fluid, thus undergoing a transition from a fluid to a semi-solid. Thus, the control challenge for MR actuators is in controlling the rheology of the material by magnetic flux. Typically the control system is based on the coil's current feedback. However, this approach based purely on the current control is not optimal since it is the magnetic stimuli that directly controls the material's yield stress and not the current. Thus, this work investigates the capability of a flux controller in handling the non-linearities of the actuator, including magnetic hysteresis. A model of an MR actuator that incorporates the magnetic hysteresis and the control coil dynamics is developed. The flux controller is tuned to handle the addition of the hysteresis effect. The obtained results show that the chosen control topology is very effective for the considered flux commands inputs.**

***Keywords*—magnetorheological actuator; hysteresis; dynamics; flux control; current control.**

I. Introduction

Magnetorheological (MR) actuators are semi-active devices that utilize the smart properties of magnetorheological fluids (MRF). MRFs are suspensions of ferromagnetic micron-size particles in a carrier oil. These particles form chain structures when subjected to an external magnetic field. The result is a yield stress change in the material and a resistance-to-flow increase. The effect is reversible, fast and of practical importance [1]. For instance, it has been utilized in semi-active automotive suspension systems based on MR dampers [2], [3], in which the properties of the smart fluid are modified to generate damping forces following the ride-changing conditions. MRF's rheology is controllable via the external magnetic field driven by a control circuit incl. a solenoid. Therefore, if the control system has the ability to influence the plant's (actuator) behavior via flux changes, its performance is improved [4]. The magnetic field is generated in a rather straightforward manner by applying a current to the solenoid's control coil, and thus, controlling the current implies the magnetic field change. However, the relationship between the input current and the flux is non-linear due to the characteristics of the magnetic circuit comprising MRF, ferromagnetic core, and other ferromagnetic components forming the actuator's structure – nonlinear permeability, magnetic saturation, magnetic hysteresis and eddy currents. Thus, a control system solely based on the current feedback is not optimal. As such, this work focuses on the influence of the hysteresis effect in MR actuators and the impact on the controller design. Briefly, the objective of this work is to assess the capability of the flux controller scheme for handling the intrinsic magnetic hysteresis effects in MR actuators. On one hand, it is evident that force control approaches may yield a better performance since they handle the force output changes directly, however, the solutions are not always possible due to sensor packaging in the actuator or the difficulty to obtain a model reliable enough and capable of handling the wide range of operating conditions of the actuator. On the other hand, a flux controller may provide a superior performance over the current controller as the flux is directly related to the force (through the magnetic flux – yield stress coupling) while the current is not [5]. Therefore, the flux controller concept may be considered an interim solution with the potential to widen the performance scope of MR actuator systems.

The structure of the study is as follows: section I provides the background information, whereas in section II relevant details of the hysteresis modeling approach are illustrated. In section III the proposed control scheme is then presented, and section IV highlights the simulation results involving the MR flux control system, and finally, in section V the main conclusions of the work are disclosed.

II. Modeling

In this work both the lumped parameter model (LPM) approach and the finite element (FE) method were used to model an MR actuator of choice. The objective is not to draw a direct comparison between the different approaches, but rather take the advantage of the LPM's simplicity in order to minimize the time-consuming disadvantages of the FE approach. The authors proceed first by building a FE model incl. magnetic hysteresis effects, then develop the reduced-order model of the solenoid. The model is tuned by fitting its response to the FE model output. The cascaded flux controller is then incorporated into the LPM. By doing this, the model's accuracy is not

too compromised while keeping the simulation time within a reasonable execution time to perform the controller's fine-tuning.

A. Finite Element Method - Vector hysteresis model

MR actuators usually do not involve complex geometries; the structures resemble typical solenoids. The modeled actuator is shown in Fig. 1. Examining this structure, by applying a current to the coil, magnetic field is induced, however, the magnetic flux is not restricted to the core, and it leaks into the fluid and the other components. Thus, one of the key challenges in modeling MR actuators is to properly model the magnetic paths given different material properties. The actuator's finite-element (FE) model was developed in Ansys Maxwell 2020 R2; some characteristics dimensions: rod diameter – 14 mm, core radius – 37.3 mm, outer cylinder's inner diameter – 46 mm; the coil window is 9.25 mm tall and 5.5 mm deep to accommodate 100 wire turns (0.51 mm), resulting in the coil resistance of appr. 1 Ω. The MR fluid is a carbonyl iron (26 % Fe vol.) based suspension, and the other components (rod, core, cylinder) are made of the ferrommagnetic alloy shown in Fig. 2a. Fig. 2b shows the magnetization curve of the MR fluid. The effect of hysteresis is accounted for by means of the vector hysteresis model in [6] assuming the alloy material's coercivity of 165 A/m. In this study the model is a foundation for generating the tuning data for the lumped parameter model of the actuator. The actuator model was driven by applying step voltage inputs to the coil. The step pulse periods was 600 ms period with the 50 % duty cycle, allowing the model to reach steady-state conditions. The amplitude of the excitation was varied to capture the model response up to the maximum current equal to 5 A in 1 A increments.

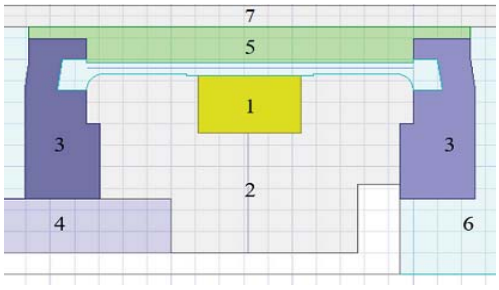

Fig. 1: MR actuator's model [5]; 1–coil, 2–ferromagnetic core, 3–plates, 4–rod, 5–sleeve, 6–MRF, 7–cylinder

B. Lumped Parameter Modeling – Jiles-Atherton Hysteresis

The LPM model was implemented in the Simcenter AMESIM simulation tool. In the essence, the model is a network of reluctances calculated based on the material's magnetisation characteristics and the core's geometry. The response of the LPM model was fitted to the results obtained from the FE hysteresis model. Figure. 3 shows the layout of the LPM AMESIM model. In order to incorporate the magnetic hysteresis, the authors used the well-known J-A model [7], [8].

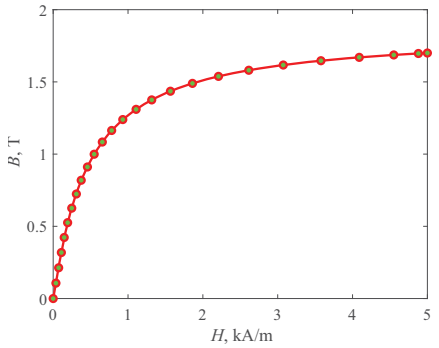

(a) Steel alloy

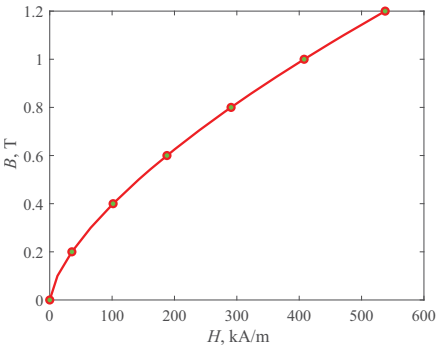

(b) MRF

Fig. 2: Magnetisation curves: $B - H$

In [9] the J-A model was used for capturing the behaviour of an MR damper at frequencies up to 10 Hz. The model consists of the following set of equations

$$\begin{cases} H_{eff} = H + \alpha M \\ M_{an} = M_s \tanh \frac{H_{eff}}{a} \\ \frac{\mathrm{d}M_{irr}}{\mathrm{d}H} = \frac{M_{an} - M_{irr}}{k\delta - \alpha(M_{an} - M_{irr})} \\ M_{rev} = c(M_{an} - M_{irr}) \\ M = M_{rev} + M_{irr} \end{cases} \tag{1}$$

where H_{eff} is the effective magnetic field, H is the applied magnetic field, M is the total magnetization, which is the sum of the reversible magnetization M_{rev} and the irreversible magnetization M_{irr}, and M_{an} is the anhysteretic magnetization. One of the advantages of the model is that it is easily tunable. By using the model parameters α, a, k, δ, and c it is possible to tune the model to match the output of the FE model. Setting up the model required two steps: 1) fitting the J-A model to match the magnetisation curve of the steel alloy, 2) fine-tuning of both the current and the flux output when subjected to the open loop excitations. The results are shown in Fig. 4; the obtained J-A model parameters were $\alpha = 0.00168$, $a = 2798.416$ A/m, $c = 0.8$, $k = 449.26$ A/m.

III. Sequential Control Scheme

The MR fluid's yield stress properties are related to the magnetic field applied to it, however, the actuator does not generate the magnetic field directly as it is in the case of

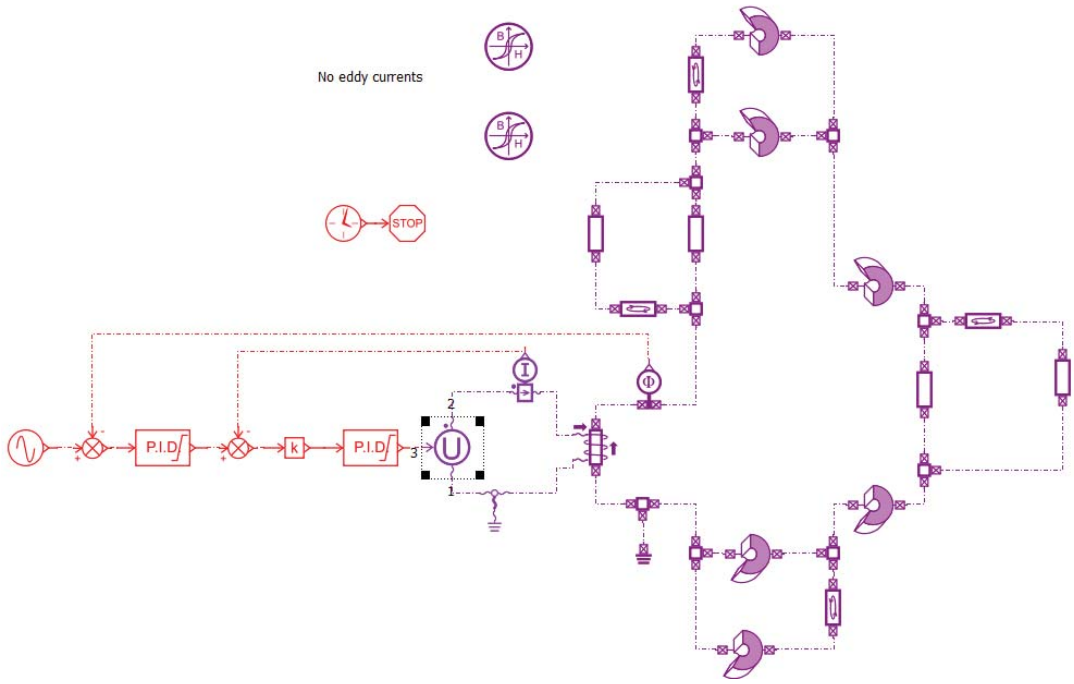

Fig. 3: AMESIM model: solenoid and controller

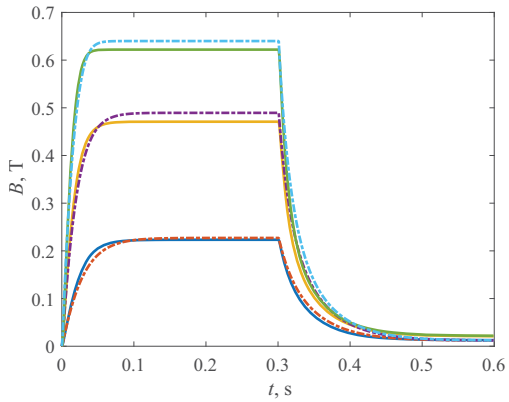

Fig. 4: Model output comparison: gap flux density

permanent magnets, but rather generates a magnetic field by injecting a current into the coil, thus generating the magnetic field. So, by controlling the current one acquires the ability to influence the magnetic flux induced in the actuator's structure. The relationship between the current and the flux, however, is not linear, given the existing phenomena e.g., magnetic hysteresis, eddy currents and the like. Previously [5], the authors proposed a control scheme for MR actuators incorporating two cascaded PI controllers. Briefly, the first driver takes the input flux, and then computes the current command, i.e. the input for the second (current) controller. Finally, the current controller provides the voltage across the coil terminals given the current command at the input of the second controller. With this approach the controller is capable to ensure that the desired flux magnitude of the MR fluid is driven to zero, which would not be possible by using just a single current controller. The concept relies on 'sensing' the magnetic flux in the actuator via measurements or model-based sensorless techniques.

IV. Results

In the essence, the flux controller would offer an improved performance over the more conventional current controller. Therefore, first, in the section the current controller results are presented. They are then followed by the data involving the flux controller subjected to the following control scenarios: bi-polar and uni-polar flux command inputs. The results are presented in Figs. 5 to 9.

A. Current controller

The performance of the solenoid driven by the PI current controller can be observed in Fig. 5. The controller was modeled using the proportional gain $K_p = 50$ and the integral gain $K_i = 100$ with the output limited to ± 12.5 V. The current command i_{cmd} was a sinusoidal current waveform, $i_{cmd}(t) = I_{cmd} \sin 2\pi f t$, where I_{cmd} is the current input amplitude, and f is the frequency. The amplitude of the command input varied from 1 A to 5 A in 1 A increments. The input frequency was set to $f = 1$ Hz from which it is possible to neglect eddy currents in the model. It seems the control system performs well and the computed error $e = i_{cmd} - i$ is small; the largest discrepancies of less than 0.1 A occur at the 5 A output peak points. However, the $B - i$ plot in Fig. 5c shows the hysteresis of appr. 0.25 A at 0 T, which is one of the main drawbacks of this controller.

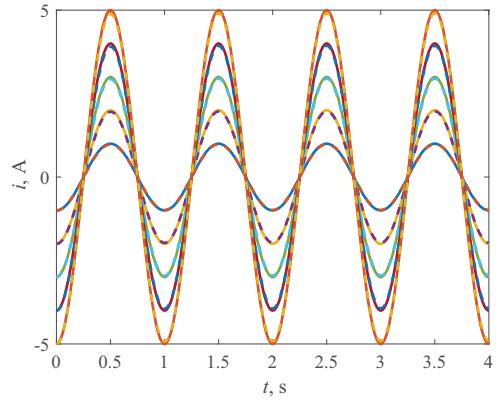

(a) $i - t$

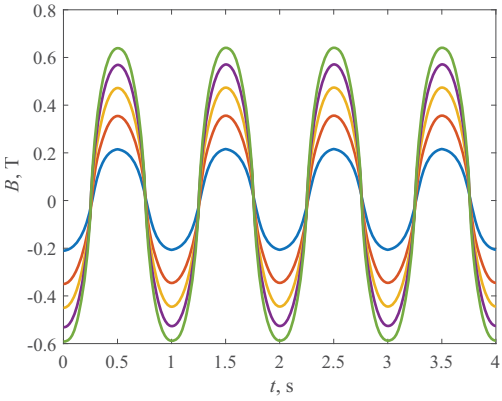

(b) $B - t$

(c) $B - i$

Fig. 5: Time history: a) measured (and commanded) current, b) gap flux density, c) gap flux density vs measured current

B. Flux controller

The flux control system's diagram is highlighted in Fig. 3. The control system behaviour was simulated in a manner similar to the one previously described. The input to the model was the magnetic flux command ϕ_{cmd} in the form of a bi-polar or a uni-polar sine wave. In the bi-polar case the input signal was $\phi_{cmd}(t) = \Phi_{cmd}\sin(2\pi ft)$, whereas in the uni-polar scenario the input command was equal to $\phi(t) = \Phi_{cmd}(1+\sin 2\pi ft)/2$, Φ_{cmd} – magnetic flux command. Additionally, the uni-polar scenario involved periodic step inputs of the same amplitude Φ_{cmd}. Finally, the controller model in Fig. 3 was tuned to yield the flux driver settings: $K_{pf} = 1$, $K_{if} = 4$. The current driver of the flux controller has the same settings as the current controller of the previous subsection.

Bipolar flux command: In this scenario the input of the control system is driven by the bipolar flux command signal $\phi(t)$. The results of the simulations are presented in Figs. 6 as time histories of magnetic flux, coil current and plots of the commanded flux input ϕ_{cmd} vs the output flux ϕ. It is evident here that the flux control approach yields an improved performance over the current controller. Not only it follows the prescribed flux command but cancels any residual flux – see Fig. 6c.

Unipolar flux command: For the sake of the comparison, the previous studies were followed by unipolar flux command scenarios. The performance of the control system under these excitations is more important as the MR fluid reacts to the absolute value of the magnetic flux in the actuator's control gap. The simulation results are shown in Figs. 7 (square wave flux command) and 8 (sine wave flux command input). Again, the illustrations reveal the good performance of the examined concept. The output flux follows the input command signal trajectory. The initial discrepancy at $t = 0$ s as seen in Fig. 8c is due to the different initial conditions and it is well reduced within 2-3 ms. Finally, the testing involved increasing the hysteresis loop width and subjecting it to the same scenarios to validate the controller's robustness. As seen in Fig. 9 the controllers achieve comparable performance without modifying the gains.

V. Conclusion

The purpose of this study was to demonstrate the magnetic flux control scheme dedicated for MR actuators taking into account the effects of magnetic hysteresis. To accomplish this, a lumped parameter electromagnetic model of the MR actuator incl. the hysteresis effect was developed. The model's output was tuned to match the response of the finite-element transient model of the MR actuator. The proposed controller concept and the lumped parameter model were then subject to extensive simulations to assess the proposed control scheme. From the obtained results, it is evident that the flux controller presents a superior performance over the conventional current controller regardless the magnitude of the excitation and the input waveform shape; the current controller would not be able to reach zero flux and would face problems to track periodic scenarios in which the hysteresis effects are more prominent.

The study goes beyond the findings of the previous research [5] by including the previously omitted magnetic hysteresis contribution. Finally, the authors plan to develop a model of the actuator that incorporates all relevant effects, e.g. eddy currents, temperature, and mechanical loads, validate it experimentally and implement the control scheme concept in the hardware.

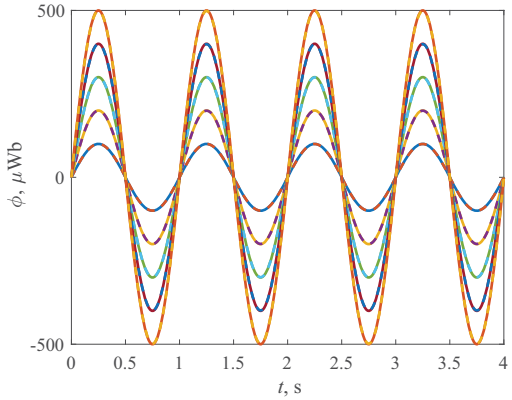

(a) $\phi - t$

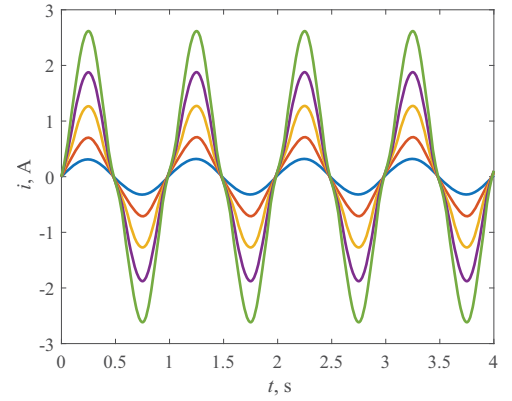

(b) $i - t$

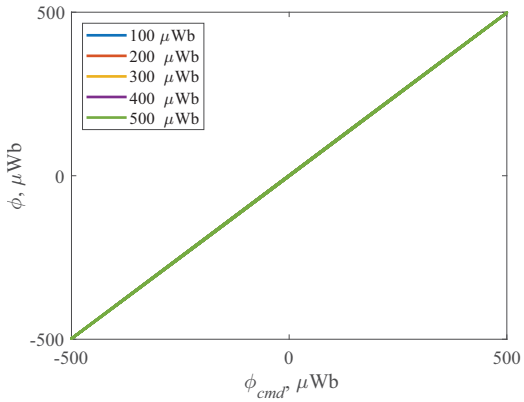

(c) $\phi - \phi_{cmd}$

Fig. 6: Output: a) measured (and commanded) flux time history, b) coil current time history, c) flux vs flux command

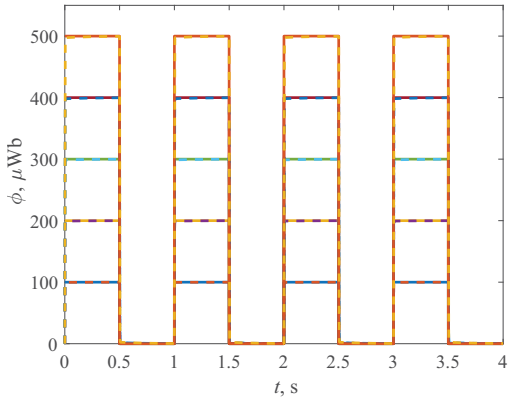

(a) $\phi - t$

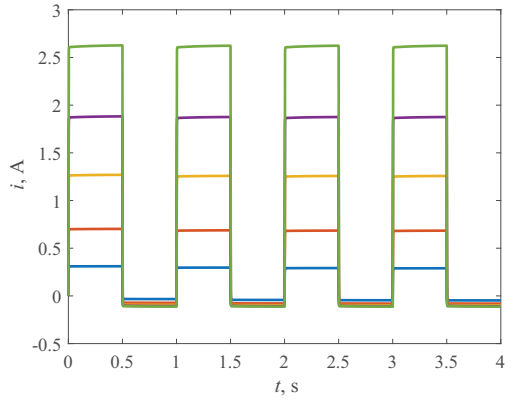

(b) $i - t$

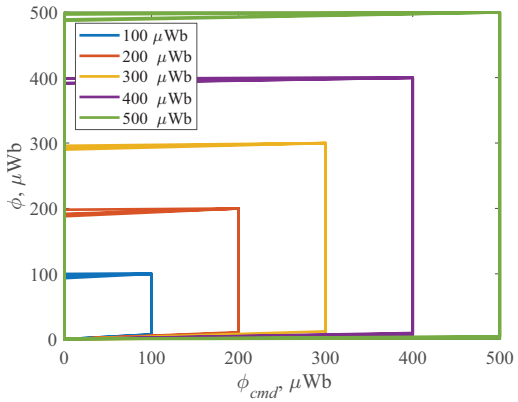

(c) $\phi - \phi_{cmd}$

Fig. 7: Output: a) measured (and commanded) flux time history, b) coil current time history, c) flux vs flux command

REFERENCES

[1] J. de Vicente, D. J. Klingenberg, and R. Hidalgo-Alvarez, "Magnetorheological fluids: a review," *Soft Matter*, vol. 7, no. 8, p. 3701, 2011. [Online]. Available: http://xlink.rsc.org/?DOI=c0sm01221a

[2] M. Belkacem, K. Z. Meguenni, and I. K. Bousserhane, "Comparative study between backstepping and backstepping sliding mode controller for suspension of vehicle with a magneto-rheological damper," *International Journal of Power Electronics and Drive Systems (IJPEDS)*, vol. 13, no. 2, p. 689, Jun. 2022. [Online]. Available: http://ijpeds.iaescore.com/index.php/IJPEDS/article/view/21639

[3] H. Du, J. Lam, K. C. Cheung, W. Li, and N. Zhang, "Direct voltage control of magnetorheological damper for vehicle suspensions," *Smart Materials and Structures*, vol. 22, no. 10, p. 105016, Oct. 2013. [Online]. Available: https://iopscience.iop.org/article/10.1088/0964-1726/22/10/105016

[4] B. K. Kumbhar, S. R. Patil, and S. M. Sawant, "Synthesis and characterization of magneto-rheological (MR) fluids for MR brake application," *Engineering Science and Technology, an International Journal*, vol. 18, no. 3, pp. 432–438, Sep. 2015. [Online]. Available: https://linkinghub.elsevier.com/retrieve/pii/S2215098615000348

[5] G. Mendes and J. Goldasz, "Advances in the Control Schemes for MR Actuators," in *2022 23rd International Carpathian Control Conference (ICCC)*. Sinaia, Romania: IEEE, May 2022, pp. 277–281. [Online]. Available: https://ieeexplore.ieee.org/document/9805907/

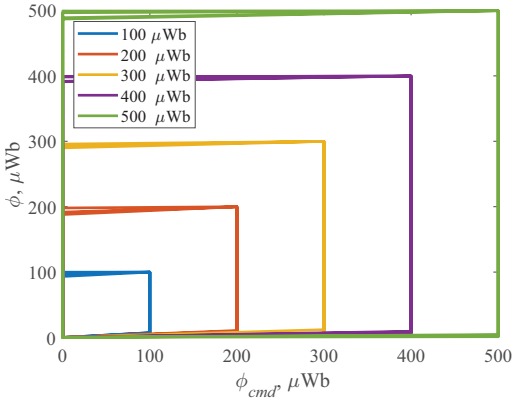

(a) $\phi - t$

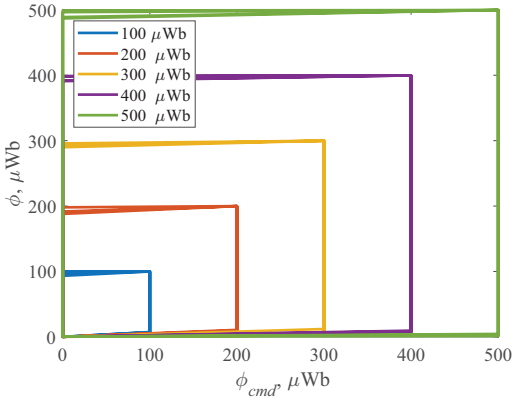

(b) $i - t$

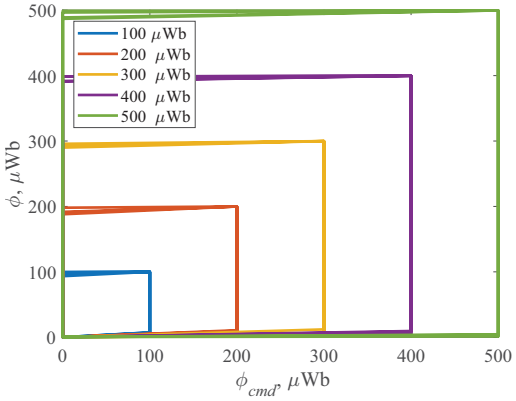

(c) $\phi - \phi_{cmd}$

Fig. 8: Time history: a) measured (and commanded) flux time history, b) coil current time history, c) flux vs flux command

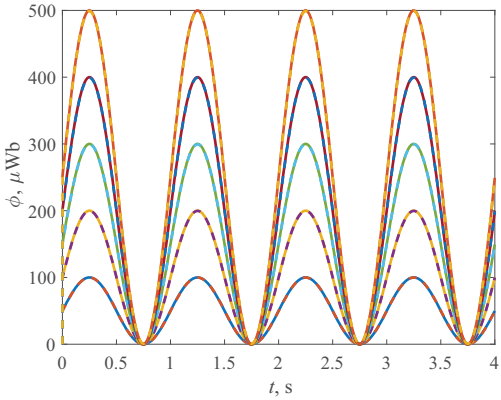

(a) $\phi - t$

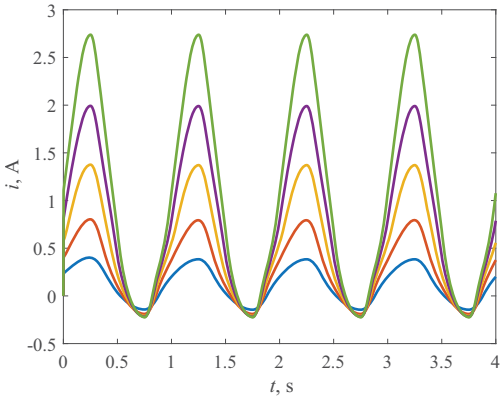

(b) $i - t$

Fig. 9: Effect of hysteresis loop width – time histories: a) measured (and commanded) flux, b) coil current

[6] D. Lin, P. Zhou, and A. Bergqvist, "Improved Vector Play Model and Parameter Identification for Magnetic Hysteresis Materials," *IEEE Transactions on Magnetics*, vol. 50, no. 2, pp. 357–360, Feb. 2014. [Online]. Available: http://ieeexplore.ieee.org/document/6749115/

[7] K. Chwastek, "Modelling of dynamic hysteresis loops using the Jiles–Atherton approach," *Mathematical and Computer Modelling of Dynamical Systems*, vol. 15, no. 1, pp. 95–105, 2009, publisher: Taylor & Francis _eprint: https://doi.org/10.1080/13873950802432016. [Online]. Available: https://doi.org/10.1080/13873950802432016

[8] A. Raghunathan, Y. Melikhov, J. Snyder, and D. Jiles, "Modeling the Temperature Dependence of Hysteresis Based on Jiles–Atherton Theory," *IEEE Transactions on Magnetics*, vol. 45, no. 10, pp. 3954–3957, Oct. 2009. [Online]. Available: http://ieeexplore.ieee.org/document/5257370/

[9] P. Guo, J. Xie, and X. Guan, "Dynamic Model of MR Dampers Based on a Hysteretic Magnetic Circuit," *Shock and Vibration*, vol. 2018, pp. 1–13, 2018. [Online]. Available: https://www.hindawi.com/journals/sv/2018/2784950/